

# Global Precipitation Trends across Spatial Scales Using Satellite Observations

PHU NGUYEN, ANDREA THORSTENSEN, SOROOSH SOROOSHIAN, KUOLIN HSU, AMIR AGHAKOUCHAK, HAMED ASHOURI, HOANG TRAN, AND DAN BRAITHWAITE

Changes in precipitation patterns are highly related to variability of atmospheric circulations, which can be influenced by a warming climate [e.g., shifts in storm tracks (Trenberth 2011)], leading to an increasing trend in global precipitation (Ren et al. 2013). As possible causes, some suggest an increase in hydrologic extremes (Karl and Knight 1998; Groisman et al. 2005; Alexander et al. 2006; Westra et al. 2013) in response to a warming climate, while others propose location-specific intensification of the global hydrologic cycle, where the wet regions get wetter and the dry regions get drier (Held and Soden 2006). At the same time, there is little evidence provided by historical observations supporting the notion that the wet gets wetter and the dry gets drier (Greve et al. 2014). Furthermore, to achieve any semblance of understanding of global historical precipitation trends, spatial aggregation of precipitation is necessary (Fischer et al. 2013). In fact, the conversation of global hydrometeorological response to climate change often has taken shape around political concerns or national security foci such as food (Rosenzweig and Parry 1994), water resources, or hazard mitigation (e.g., flood and drought), and are typically spatially confined by

political or jurisdictional boundaries. Therefore, the flexibility to shape historical precipitation analysis to meet the requirements of this conversation is of the utmost importance. In the absence of long-term global precipitation observations, little can be said with confidence in terms of global precipitation trends (Gruber and Levizzani 2008). An initial effort in this direction can be found in previous studies that examine precipitation at both regional and global scales (Wu and Fu 2013) or investigate simulated precipitation response with changing model resolution (Rasmussen et al. 2012; Mendoza et al. 2016). However, these studies are interested in model result implications. Those that do emphasize observations tend to focus on a single geographical area at a regional scale as a compliment to a single form of global analysis, rather than shaping the global discussion around varying methods of spatial division. Other studies (Adler et al. 2017; Gu et al. 2016; Wang et al. 2016; Gu and Adler 2013) use the Global Precipitation Climatology Project (GPCP) at 2.5° resolution to investigate global precipitation trends, but they lack the high resolution needed to do so at varying spatial scales. This is especially important for divisions with highly irregular borders such as political boundaries and watersheds.

A recently released high-resolution global precipitation dataset from NOAA—Precipitation Estimation from Remotely Sensed Information using Artificial Neural Networks—Climate Data Record (PERSIANN-CDR; Ashouri et al. 2015)—provides the ability to reexamine and gain new insights about the global precipitation trends across different spatial scales. PERSIANN-CDR was developed based on the artificial neural network model named PERSIANN (Hsu et al. 1997; Sorooshian et al. 2000). PERSIANN-CDR uses brightness temperature retrievals of infrared information from geostationary Earth-orbiting satellites to estimate rainfall and the monthly GPCP rain gauge observations for bias correction. Various validations

**AFFILIATIONS:** NGUYEN—Center for Hydrometeorology and Remote Sensing, and Department of Civil and Environmental Engineering, University of California, Irvine, Irvine, California, and Nong Lam University, Ho Chi Minh City, Vietnam; THORSTENSEN, SOROOSHIAN, HSU, AGHAKOUCHAK, ASHOURI, TRAN, AND BRAITHWAITE—Center for Hydrometeorology and Remote Sensing, and Department of Civil and Environmental Engineering, University of California, Irvine, Irvine, California  
**CORRESPONDING AUTHOR:** Phu Nguyen, ndphu@uci.edu

DOI:10.1175/BAMS-D-17-0065.1

©2018 American Meteorological Society  
For information regarding reuse of this content and general copyright information, consult the [AMS Copyright Policy](#).

have shown the usefulness of PERSIANN-CDR for climate studies (Miao et al. 2015; Luchetti et al. 2016; Ashouri et al. 2016).

This study offers new insights on global precipitation trends across different spatial scales, using the recently developed RainSphere (Nguyen et al. 2017; <http://rainsphere.eng.uci.edu>) tool, which allows for spatial analysis of historical precipitation observations using the PERSIANN-CDR dataset. A unique feature of RainSphere is that it allows for examining trends from pixel scale to global scale using spatially homogeneous satellite-based precipitation observations.

**METHOD.** We used the PERSIANN-CDR precipitation estimates (Ashouri et al. 2015) to investigate the trend in the mean annual precipitation at different spatial scales, from a  $0.25^\circ \times 0.25^\circ$  grid cell to country level, to continental level, and to climate zones. PERSIANN-CDR is a long-term (33+ years from 1983 to present) high-spatiotemporal-resolution ( $0.25^\circ$ , daily) precipitation product, maintained and distributed at the National Oceanic and Atmospheric Administration (NOAA)'s National Centers for Environmental Information (NCEI, [www.ncdc.noaa.gov/cdr/atmospheric/precipitation-persiann-cdr](http://www.ncdc.noaa.gov/cdr/atmospheric/precipitation-persiann-cdr)). PERSIANN-CDR uses merged infrared images from multisatellite observations in a trained neural-network framework using the PERSIANN algorithm. The resulting precipitation estimates are then bias corrected using the Global Precipitation Climatology Project (GPCP) monthly product.

We used the same statistical method for trend analysis as used in the RainSphere system (Nguyen et al. 2017). We implemented the daily PERSIANN-CDR dataset in a PostGIS database, which allows for querying spatial and temporal patterns of precipitation.

We used the nonparametric test method developed by Mann–Kendall (Mann 1945; Kendall 1976) for trend analysis. We calculated  $S$  statistics to identify the sign (negative for decreasing and positive for increasing) and magnitude of the trend in each time series of precipitation data and then determined whether the trend was significant or not.

The  $S$  value of a time series precipitation variable  $X(x_1, x_2, \dots, x_n)$  can be calculated as follows:

$$S = \sum_{k=1}^{n-1} \sum_{j=k+1}^n \text{sgn}(x_j - x_k),$$

where  $\text{sgn}$  is the sign function:

$$\text{sgn}(x_j - x_k) = \begin{cases} +1 & \text{if } (x_j - x_k) > 0 \\ 0 & \text{if } (x_j - x_k) = 0. \\ -1 & \text{if } (x_j - x_k) < 0 \end{cases}$$

For a better illustration of the rainfall trends we normalized the  $S$  value to  $[-1, 1]$ .

We tested the null hypothesis  $H_0$  that there is no significant trend in the data at significance level  $\alpha = 0.05$  (or 95% confidence level). The significance of a trend can be estimated using a  $z$  test (Yue et al. 2002; Damberg and AghaKouchak 2014):

$$z = \begin{cases} \frac{S - 1}{\sqrt{\frac{n(n-1)(2n+5)}{18}}} & \text{if } S > 0 \\ 0 & \text{if } S = 0 \\ \frac{S + 1}{\sqrt{\frac{n(n-1)(2n+5)}{18}}} & \text{if } S < 0 \end{cases}$$

The  $p$  value is defined as the probability of obtaining the data values under the null hypothesis that there is no trend (Fatichi 2009). The null hypothesis  $H_0$  is accepted (i.e., there is no significant trend in the data) if the  $p$  value is larger than  $\alpha$ , while there is a significant trend if the  $p$  value is smaller than  $\alpha$  where

$$p = 0.5 - \frac{1}{\sqrt{2\pi}} \int_0^z e^{-t^2/2} dt.$$

**RESULTS. Global pixel-based scale.** Figure 1 shows the annual mean and pixel-based trends of global precipitation from 1983 to 2015 from the PERSIANN-CDR dataset. Globally ( $60^\circ\text{N}$ – $60^\circ\text{S}$ ), we are observing 2.36% statistically significant increasing, 42.84% insignificant increasing, 4.48% significant decreasing, and 48.44% insignificant decreasing trend in the mean annual precipitation for 1983–2015 (all at 0.05 significance level). These trend percentages are, respectively, 2.95%, 49.74%, 2.93%, and 42.37% over the land, and 2.14%, 40.26%, 5.07%, and 50.71% over the ocean.

**Continental scale.** Figure 2 shows the changes in precipitation volume over oceans and continents during the past 3 decades. As shown in Figs. 2b and 2c, fluctuations are present in the total amount of

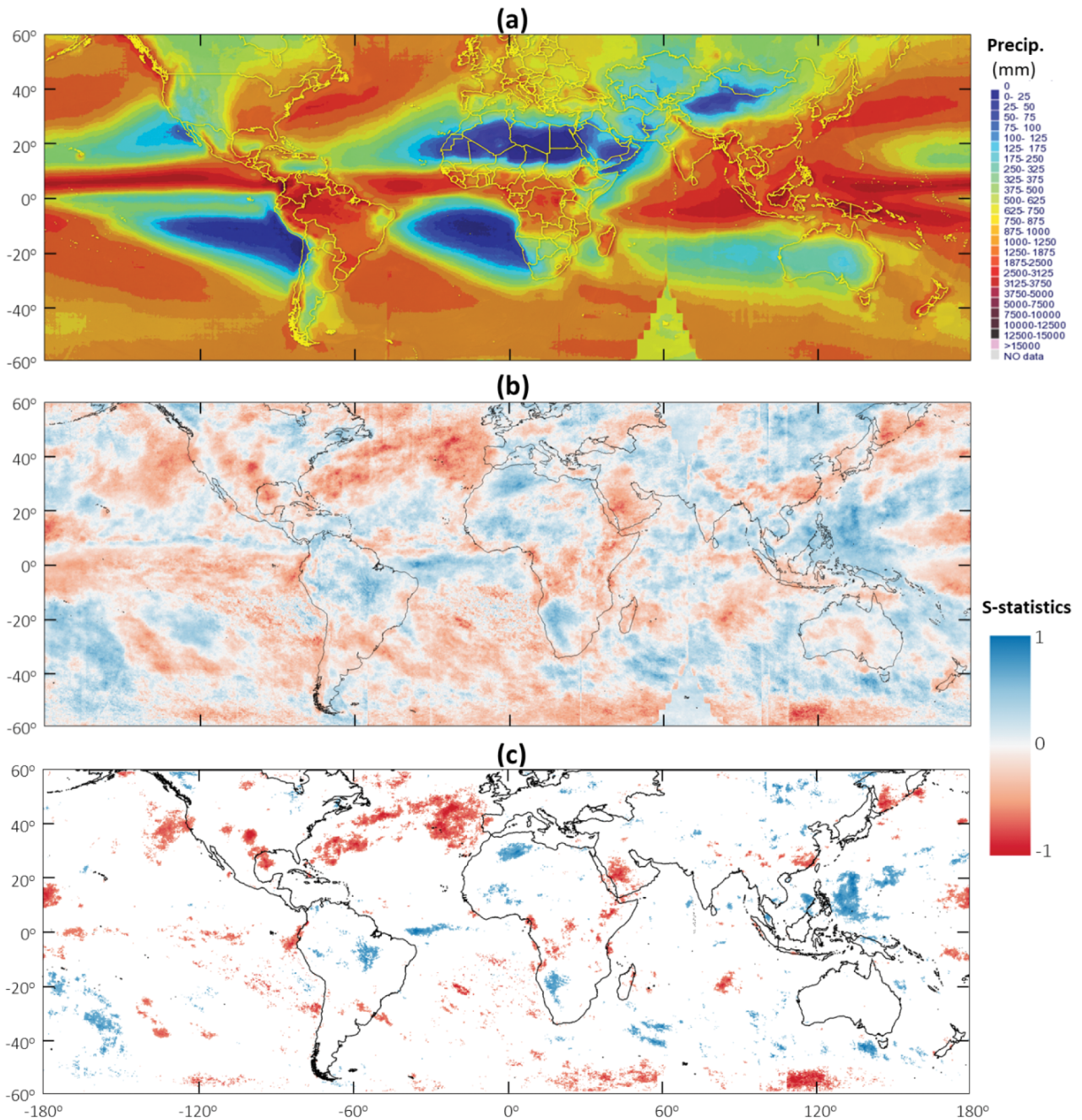


**FIG. 1. Global precipitation trends. (a) Annual mean precipitation in mm, and (b),(c) pixel-based precipitation trends from 1983 to 2015 from PERSIANN-CDR. In (b) and (c) the warm colors show a decreasing trend and the cool colors show an increasing trend in precipitation. Note (c) only shows the S statistics at pixels where the observed trend is statistically significant at the 0.05 significance level according to the Mann–Kendall test.**

precipitation that has fallen over land and ocean; however, no significant long-term volumetric change is observed for either case. As shown in Fig. 2a, the mean annual precipitation over the Atlantic has been decreasing statistically significantly in response to

the robust decrease in precipitation over the North Atlantic Ocean. The increase in precipitation in the western Pacific Ocean cancels out part of the positive trend in the eastern Pacific, resulting in an overall insignificant negative trend in the Pacific Ocean rainfall.

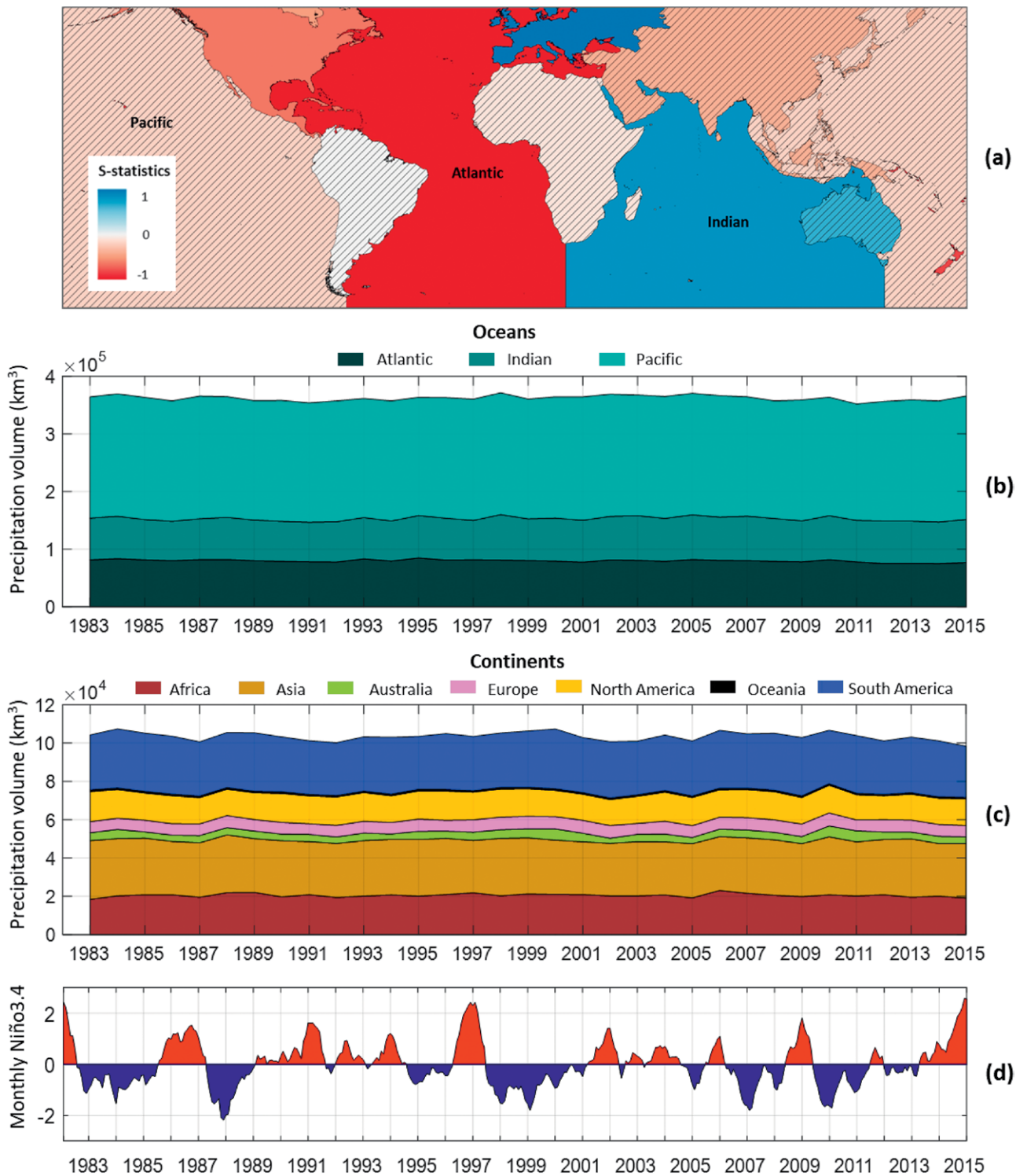
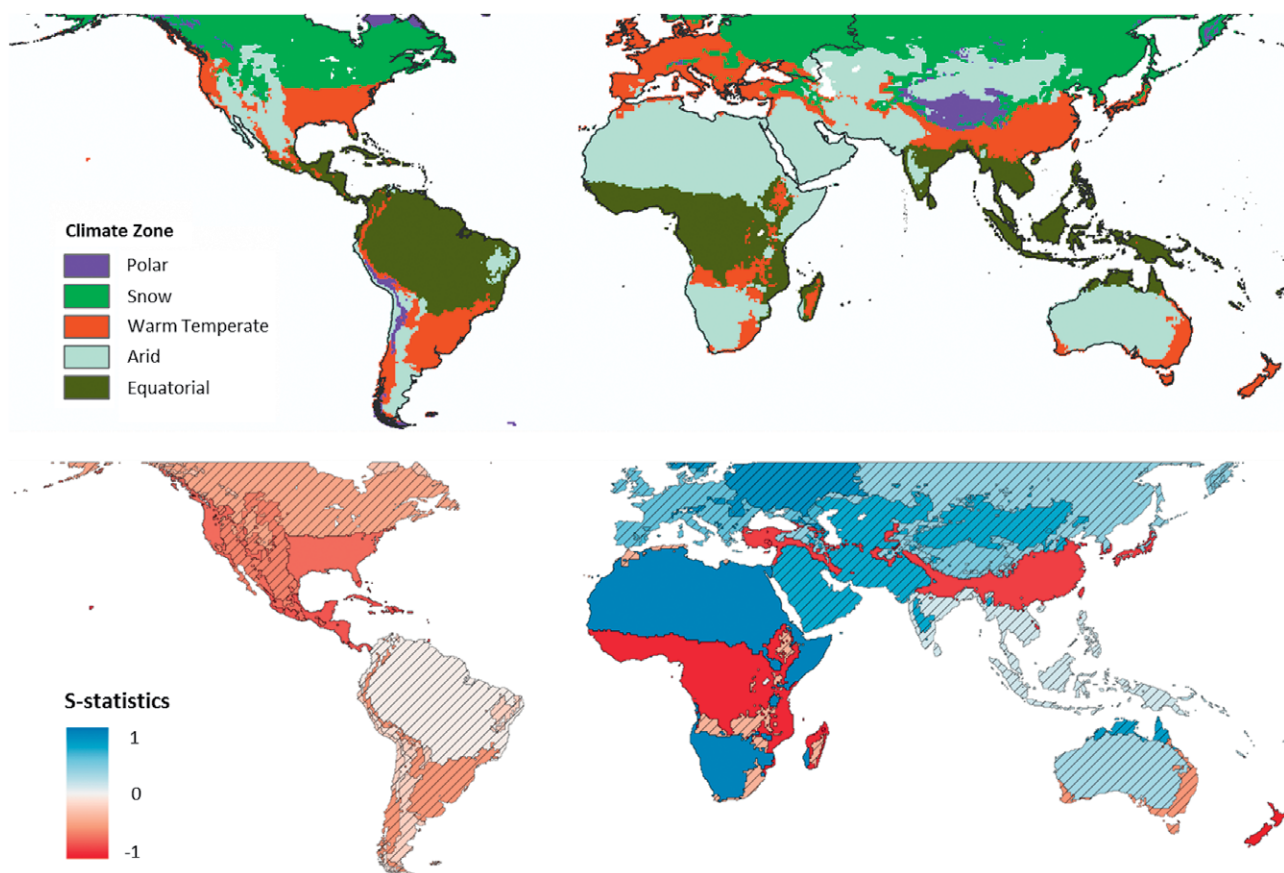


**FIG. 2. Continental and oceanic trends. (a) Precipitation volume trends over continents and oceans, (b),(c) changes in precipitation volume, and (d) monthly Niño-3.4. In (a), warm and cool colors, respectively, show decreasing and increasing trends, and shaded areas have no significant trends according to the Mann–Kendall test.**

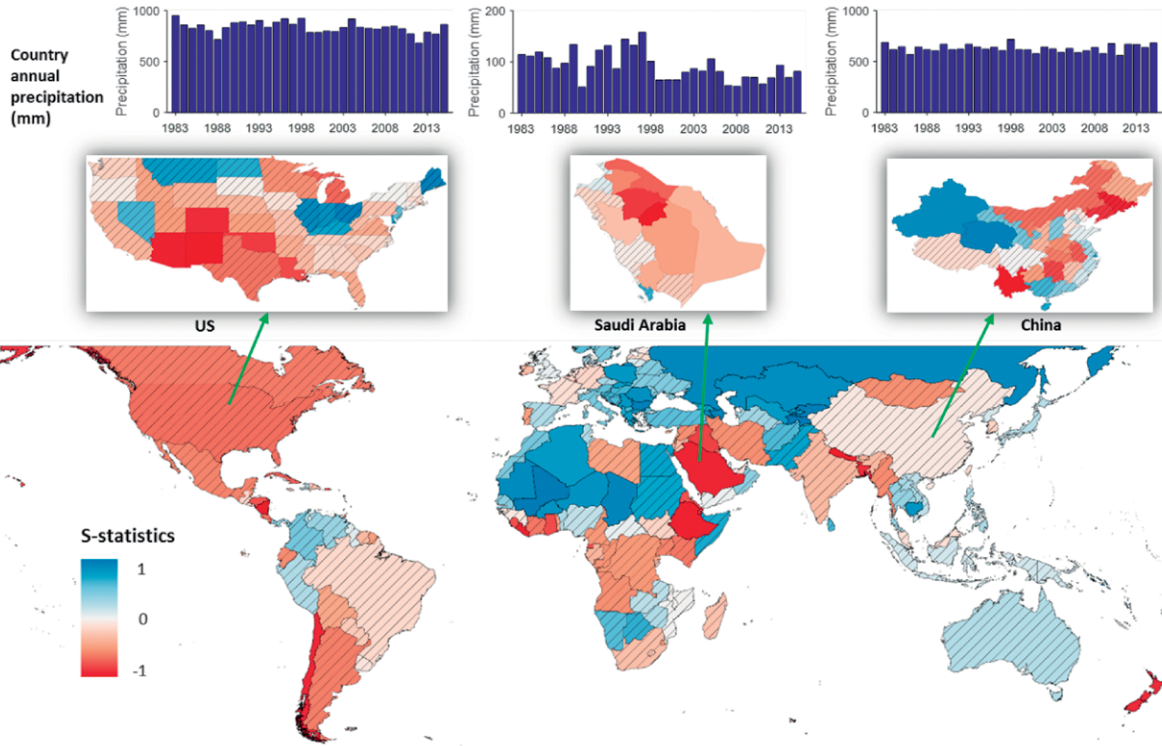
North America and Oceania have been experiencing significant decreasing trends in precipitation, while the trend is the opposite over Europe (Fig. 2a).

Figure 2d shows the monthly Niño-3.4 index from the NOAA Climate Prediction Center (CPC). For most of the continents, there are inverse relationships between the 12-month-average Niño-3.4 and total yearly rainfall volumes, except for North America. Specifically, these correlations (significance values) are  $-0.401$  ( $0.021$ ) for Africa,  $-0.382$  ( $0.028$ ) for Asia,  $-0.456$  ( $0.008$ ) for Australia,  $-0.122$  ( $0.497$ ) for Europe,  $0.106$  ( $0.557$ ) for North America,  $-0.355$  ( $0.043$ ) for Oceania, and  $-0.540$  ( $0.001$ ) for South America. The statistics show that there is more precipitation during the La Niña years and less precipitation during the El Niño years globally over land, with correlation and significance value between the 12-month-average Niño-3.4 and total yearly rainfall volumes being  $-0.733$  and  $0.000$ , respectively.

*Climate zones.* We used the Köppen–Geiger climate classification map (available at <http://koeppen-geiger.vu-wien.ac.at/shifts.htm>) to define the boundaries of five global climate zones—polar, snow, warm temperate, arid, and equatorial (Fig. 3a). These groups were further classified by each continent. We then investigated how the precipitation trends vary over each of these climate zone–continent groups. The unshaded regions in Fig. 3b depict the regions where the precipitation trend is statistically significant. As shown, the warm temperate regions in North America and East Asia, as well as the equatorial regions in Africa, have been experiencing statistically significant negative trends in their mean annual precipitation. On the contrary, arid regions over Africa are observing a positive precipitation trend. In general, warm temperate climate regions have decreasing trends while arid and polar climate regions have increasing trends in precipitation. Africa shows the clearest precipitation



**FIG. 3. Trend in climate zones. Precipitation trends from 1983 to 2015 over climate zone–continent groups (60°N–60°S). The colors indicate S statistics values. Warm and cool colors, respectively, show decreasing and increasing trends. Shaded areas have no significant trends according to the Mann–Kendall test.**



**FIG. 4. Country-scale trends. Precipitation trends from 1983 to 2015 over 201 countries (60°N–60°S) and state/province political divisions of the United States, Saudi Arabia, and China. The colors indicate the S statistics values. Warm and cool colors, respectively, show decreasing and increasing trends. Shaded areas have no significant trends according to the Mann–Kendall test.**

trends according to climate zones, where arid regions have a significant increase and the equatorial region has a significant decreasing trend.

*Political divisions.* Following our analyses of the mean annual precipitation trends at different spatial scales, we investigated the existence of such trends across different political divisions, globally. Figure 4 shows that, out of 201 countries, mean annual precipitation for 20 countries exhibits significant increasing trends, while for 24 countries it shows significant decreasing trends. Likewise, the mean annual precipitation for 76 countries shows insignificant increasing trends and for 80 countries insignificant decreasing trends. Within a country there can be different precipitation trends over the state/province level. In Fig. 4, we also zoom into three countries for more details. The United States as a whole has a statistically insignificant decreasing trend. However, when zooming into the state level, we can see that Arizona, New Mexico, Colorado, Oklahoma, and Louisiana have significantly decreasing trends, whereas Nevada, Montana, North Dakota, Illinois, Indiana, Kentucky, and Ohio have increasing trends

that are not statistically significant. Saudi Arabia in its entirety has a significant decreasing trend, and most of its provinces have decreasing trends. In China, regions with increasing trends cancel out regions with decreasing trends in the northwest and coastal southeast, resulting in no obvious trend for the whole country. Using RainSphere, the user community can investigate the precipitation patterns of their countries of interest both at the country and the state/province levels.

*Water resources management.* We often see reports based on country boundaries; however, the real answer to precipitation trends and variations may be outside political boundaries. Therefore, it is imperative to extend our analysis beyond political divisions and investigate precipitation trends for water resources management units (major basin level). Figure 5 shows the precipitation trends over 237 global major basins. Globally, 20 basins have significant increasing trends and 20 basins have significant decreasing trends in precipitation. Additionally, 89 basins have insignificant increasing trends and 106 basins have insignificant decreasing trends in precipitation.

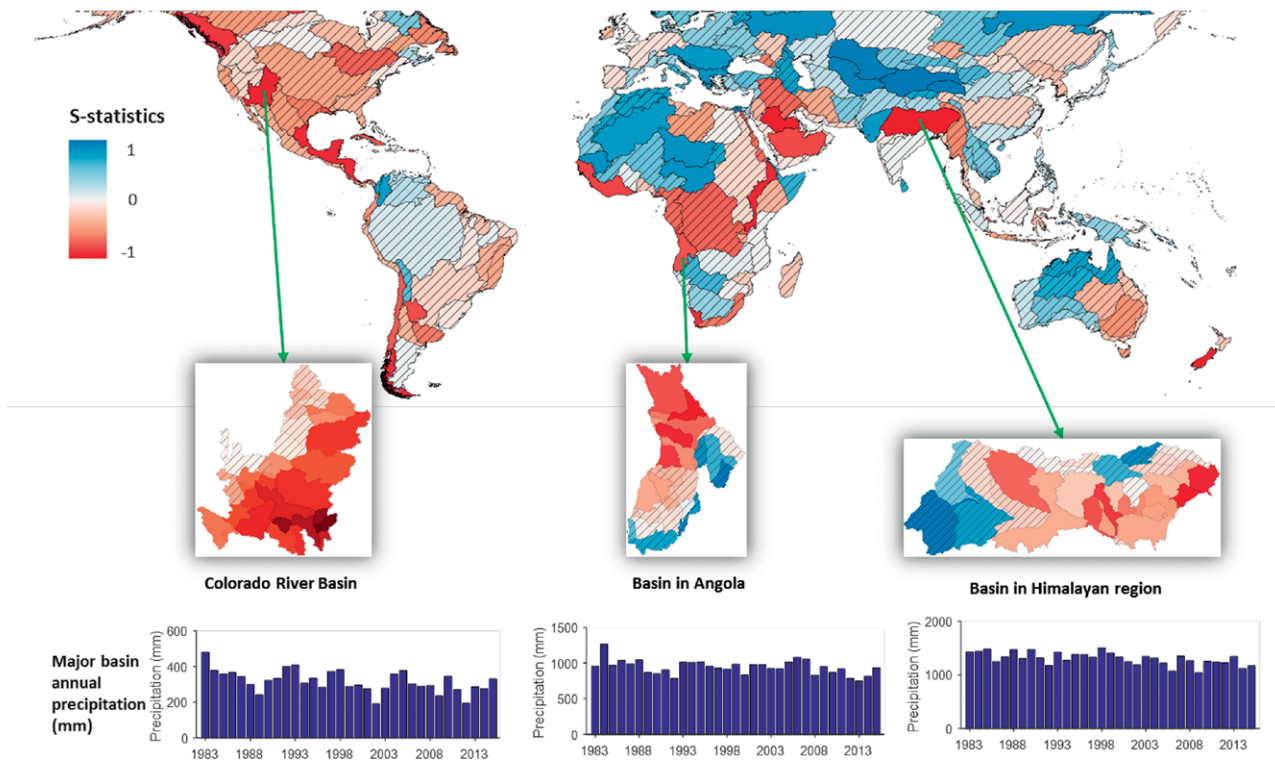


**FIG. 5. Basin-scale trends.** Precipitation trends from 1983 to 2015 over 237 global major basins (60°N–60°S) and detailed watersheds of the Colorado River basin, the basin in Angola, and the basin in the Himalayan region. The colors indicate *S* statistics values. Warm and cool colors, respectively, show decreasing and increasing trends. Shaded areas have no significant trends according to the Mann–Kendall test.

RainSphere gives the user community the tools to further narrow down the basin-level analyses and look into precipitation trends at a watershed level. For instance, as shown in Fig. 5, the Colorado River basin has been experiencing a decreasing trend, with most of its watersheds having significant decreasing trends, while the watersheds in the Angola and Himalayan regions show both decreasing and increasing trends even though they both have significant decreasing trends in precipitation as whole basins.

At the end of the day, the consequences of climate variability and change in water resources are realized at the watershed to river basin scale where people live, crops are grown, and industrial water requirements for production purposes exist. The basin and watershed boundaries are from the HydroSHEDS project (Lehner et al. 2008).

Attempting to answer the multispatial-scale perspective on the global historical precipitation trends question via RainSphere presents a bevy of (sometimes conflicting) conclusions about the hydrometeorological response to past climate change. A global pixel-by-

pixel trend analysis reveals select areas with statistically significant volumetric precipitation trends such as the northern Atlantic (decreasing) and northern Africa (increasing). However, the message changes dramatically in some areas when the stringency of precise pixel location for trend analysis is removed. For instance, in the case of both Europe and the Indian Ocean, a mixed historical precipitation trend pattern is present, but when taken as an aggregated spatial area a statistically significant increasing trend emerges for these regions. The story changes further still as subboundaries are defined and opposite trends may nullify each other at the larger scale, or small areas with strong trends might dominate the larger area that otherwise exhibits no trend.

Given that many parties have a vested interest in the hydrometeorological response to global climate change, it is important to be equipped with information that adequately reflects the specific question at hand. This study highlights the complications present in historical precipitation trend analysis through examining the effects of spatial unit choice.

Generalizations about precipitation trends for the globe, continents, or even large countries have implications when delivered to decision-makers, who are often responsible for smaller spatial entities. China, for example, shows no significant trend at the national level but features two units at the provincial level that show significant and opposite trends. For the decision-makers and planners of these provinces, the information at the national level suggesting “business as usual” may not be adequate to form an appropriate response. Furthermore, the region that may be most important to a given political division in terms of water resources is not necessarily within that political boundary. In fact, the fate of the portion of a basin upstream of a region in question often has the most impact on that region and, frequently, this becomes a cross-political boundary issue. Such a strong sensitivity to the choice of area delineation begs the use of caution in selecting the proper analysis scale and boundaries.

The take-home message from our study using the new 33+ years of high-resolution global precipitation dataset is that there seems not to be any detectable and significant positive trends in the amount of global precipitation due to the now well-established increasing global temperature. While there are regional trends, there is no evidence of increase in precipitation at the global scale in response to the observed global warming. Perhaps the explanation can be that satellite data used in this study is limited to between 60°N and 60°S and any precipitation above and below these latitudes is unavailable.

**ACKNOWLEDGMENTS.** This research was partially supported by the Cooperative Institute for Climate and Satellites (CICS) program (NOAA Award NA14NES4320003, Subaward 2014-2913-03) for OHD-NWS student fellowship, the Army Research Office (Award W911NF-11-1-0422), National Science Foundation (NSF Award 1331915), and Department of Energy (DOE Award DE-IA0000018).

## FOR FURTHER READING

- Adler, R. F., and Coauthors, 2017: Global precipitation: Means, variations and trends during the satellite era (1979–2014). *Surv. Geophys.*, **38**, 679–699, <https://doi.org/10.1007/s10712-017-9416-4>.
- Alexander, L. V., and Coauthors, 2006: Global observed changes in daily climate extremes of temperature and precipitation. *J. Geophys. Res.*, **111**, D05109, <https://doi.org/10.1029/2005JD006290>.
- Ashouri, H., and Coauthors, 2015: PERSIANN-CDR: Daily precipitation climate data record from multisatellite observations for hydrological and climate studies. *Bull. Amer. Meteor. Soc.*, **96**, 69–83, <https://doi.org/10.1175/BAMS-D-13-00068.1>.
- , P. Nguyen, A. Thorstensen, K. L. Hsu, S. Sorooshian, and D. Braithwaite, 2016: Assessing the efficacy of high-resolution satellite-based PERSIANN-CDR precipitation product in simulating streamflow. *J. Hydrometeor.*, **17**, 2061–2076, <https://doi.org/10.1175/JHM-D-15-0192.1>.
- Damberg, L., and A. AghaKouchak, 2014: Global trends and patterns of drought from space. *Theor. Appl. Climatol.*, **117**, 441–448, <https://doi.org/10.1007/s00704-013-1019-5>.
- Fatichi, S., 2009: Mann-Kendall test. Tech rep., Dipartimento Ingegneria Civile e Ambientale, Università degli Studi di Firenze.
- Fischer, E. M., U. Beyerle, and R. Knutti, 2013: Robust spatially aggregated projections of climate extremes. *Nat. Climate Change*, **3**, 1033–1038, <https://doi.org/10.1038/nclimate2051>.
- Greve, P., and Coauthors, 2014: Global assessment of trends in wetting and drying over land. *Nat. Geosci.*, **7**, 716–721, <https://doi.org/10.1038/ngeo2247>.
- Groisman, P. Ya., and Coauthors, 2005: Trends in intense precipitation in the climate record. *J. Climate*, **18**, 1326–1350, <https://doi.org/10.1175/JCLI3339.1>.
- Gruber, A., and V. Levizzani, 2008: Assessment of global precipitation products: A project of the World Climate Research Programme Global Energy and Water Cycle Experiment (GEWEX) Radiation Panel. WCRP Rep. 128, WMO/TD No. 1430, 50 pp.
- Gu, G., and R. F. Adler, 2013: Interdecadal variability/long-term changes in global precipitation patterns during the past three decades: global warming and/or pacific decadal variability? *Climate Dyn.*, **40**, 3009–3022, <https://doi.org/10.1007/s00382-012-1443-8>.
- , —, and G. J. Huffman, 2016: Long-term changes/trends in surface temperature and precipitation during the satellite era (1979–2012). *Climate Dyn.*, **46**, 1091–1105, <https://doi.org/10.1007/s00382-015-2634-x>.
- Held, I. M., and B. J. Soden, 2006: Robust responses of the hydrological cycle to global warming. *J. Climate*, **19**, 5686–5699, <https://doi.org/10.1175/JCLI3990.1>.
- Hsu, K. L., X. Gao, S. Sorooshian, and H. V. Gupta, 1997: Precipitation estimation from remotely sensed information using artificial neural networks. *J. Appl. Meteor. Climatol.*, **36**, 1176–1190, [https://doi.org/10.1175/1520-0450\(1997\)036<1176:PEFRSI>2.0.CO;2](https://doi.org/10.1175/1520-0450(1997)036<1176:PEFRSI>2.0.CO;2).

- Jones, P. D., and A. Moberg, 2003: Hemispheric and large-scale surface air temperature variations: An extensive revision and an update to 2001. *J. Climate*, **16**, 206–223, [https://doi.org/10.1175/1520-0442\(2003\)016<0206:HALSSA>2.0.CO;2](https://doi.org/10.1175/1520-0442(2003)016<0206:HALSSA>2.0.CO;2).
- Karl, T. R., and R. W. Knight, 1998: Secular trends of precipitation amount, frequency, and intensity in the United States. *Bull. Amer. Meteor. Soc.*, **79**, 231–241, [https://doi.org/10.1175/1520-0477\(1998\)079<0231:STOPAF>2.0.CO;2](https://doi.org/10.1175/1520-0477(1998)079<0231:STOPAF>2.0.CO;2).
- Kendall, M., 1976: *Rank Correlation Methods*, 4th ed. Griffin, London.
- Lehner, B., K. Verdin, and A. Jarvis, 2008: New global hydrography derived from spaceborne elevation data. *Eos, Trans. Amer. Geophys. Union*, **89**, 93–94, <https://doi.org/10.1029/2008EO100001>.
- Luchetti, N. T., J. R. Sutton, E. E. Wright, M. C. Kruk, and J. J. Marra, 2016: When El Niño rages: How satellite data can help water-stressed islands. *Bull. Amer. Meteor. Soc.*, **97**, 2249–2255, <https://doi.org/10.1175/BAMS-D-15-00219.1>.
- Mann, H., 1945: Nonparametric tests against trend. *Econometrica*, **13**, 245–259, <https://doi.org/10.2307/1907187>.
- Mendoza, P. A., and Coauthors, 2016: Effects of different regional climate model resolution and forcing scales on projected hydrologic changes. *J. Hydrol.*, **541**, 1003–1019, <https://doi.org/10.1016/j.jhydrol.2016.08.010>.
- Miao, C., and Coauthors, 2015: Evaluation of the PERSIANN-CDR daily rainfall estimates in capturing the behavior of extreme precipitation events over China. *J. Hydrometeorol.*, **16**, 1387–1396, <https://doi.org/10.1175/JHM-D-14-0174.1>.
- Nguyen, P., and Coauthors, 2017: Exploring trends through “RainSphere”: Research data transformed into public knowledge. *Bull. Amer. Meteor. Soc.*, **98**, 653–658, <https://doi.org/10.1175/BAMS-D-16-0036.1>.
- Rasmussen, S. H., J. H. Christensen, M. Drews, D. J. Gochis, and J. C. Refsgaard, 2012: Spatial-scale characteristics of precipitation simulated by regional climate models and the implications for hydrological modeling. *J. Hydrometeorol.*, **13**, 1817–1835, <https://doi.org/10.1175/JHM-D-12-07.1>.
- Ren, L., P. Arkin, T. M. Smith, and S. S. Shen, 2013: Global precipitation trends in 1900–2005 from a reconstruction and coupled model simulations. *J. Geophys. Res. Atmos.*, **118**, 1679–1689, <https://doi.org/10.1002/jgra.50096>.
- Rosenzweig, C., and M. L. Parry, 1994: Potential impact of climate change on world food supply. *Nature*, **367**, 133–137, <https://doi.org/10.1038/367133a0>.
- Sorooshian, S., and Coauthors, 2000: Evaluation of PERSIANN system satellite-based estimates of tropical rainfall. *Bull. Amer. Meteor. Soc.*, **81**, 2035–2046, [https://doi.org/10.1175/1520-0477\(2000\)081<2035:EOPSSE>2.3.CO;2](https://doi.org/10.1175/1520-0477(2000)081<2035:EOPSSE>2.3.CO;2).
- Trenberth, K. E., 2011: Changes in precipitation with climate change. *Climate Res.*, **47**, 123–138, <https://doi.org/10.3354/cr00953>.
- Wang, B., and Coauthors, 2016: Decadal trends of the annual amplitude of global precipitation. *Atmos. Sci. Lett.*, **17**, 96–101, <https://doi.org/10.1002/asl.631>.
- Westra, S., L. V. Alexander, and F. W. Zwiers, 2013: Global increasing trends in annual maximum daily precipitation. *J. Climate*, **26**, 3904–3918, <https://doi.org/10.1175/JCLI-D-12-00502.1>.
- Wu, F. T., and C. B. Fu, 2013: Change of precipitation intensity spectra at different spatial scales under warming conditions. *Chin. Sci. Bull.*, **58**, 1385–1394, <https://doi.org/10.1007/s11434-013-5699-0>.
- Yue, S., P. Pilon, and G. Cavadas, 2002: Power of the Mann–Kendall and Spearman’s rho tests for detecting monotonic trends in hydrological series. *J. Hydrol.*, **259**, 254–271, [https://doi.org/10.1016/S0022-1694\(01\)00594-7](https://doi.org/10.1016/S0022-1694(01)00594-7).

# AMS Members

Give a  
great gift  
at a  
great price

Looking for the perfect present for the weather enthusiast in your life? Want to make a valuable contribution to your local library or community college?



Send a subscription to Weatherwise magazine for just \$24.95\*—That's nearly 50% off the list price!

Contact Member Services by e-mail at [amsmem@ametsoc.org](mailto:amsmem@ametsoc.org) or by phone at **617-227-2425** to place all of your Weatherwise orders today!

**Written for a general audience, Weatherwise offers a colorful and nontechnical look at recent discoveries in meteorology and climatology.**

Check out the latest table of contents at [www.weatherwise.org](http://www.weatherwise.org).

**Want your own?**  
Then order a personal subscription at the same great price.